nature chemical biology

ARTICLE

PUBLISHED ONLINE: 12 DECEMBER 2016 | DOI: 10.1038/NCHEMBIO.2253

Rewiring human cellular input–output using modular extracellular sensors

Kelly A Schwarz[1,2], Nichole M Daringer[1], Taylor B Dolberg[1,2] & Joshua N Leonard[1–4]*

Engineered cell-based therapies comprise a promising emerging strategy for treating diverse diseases. Realizing this promise requires new tools for engineering cells to sense and respond to soluble extracellular factors, which provide information about both physiological state and the local environment. Here, we report such a biosensor engineering strategy, leveraging a self-contained receptor–signal transduction system termed modular extracellular sensor architecture (MESA). We developed MESA receptors that enable cells to sense vascular endothelial growth factor (VEGF) and, in response, secrete interleukin 2 (IL-2). By implementing these receptors in human T cells, we created a customized function not observed in nature—an immune cell that responds to a normally immunosuppressive cue (VEGF) by producing an immunostimulatory factor (IL-2). Because this platform utilizes modular, engineerable domains for ligand binding (antibodies) and output (programmable transcription factors based upon Cas9), this approach may be readily extended to novel inputs and outputs. This generalizable approach for rewiring cellular functions could enable both translational applications and fundamental biological research.

Mammalian cell-based therapies comprise a promising and rapidly expanding technology, with over 1,300 clinical trials currently underway worldwide[1,2]. Most notably, engineered chimeric antigen receptor (CAR)-expressing T cells harness the capabilities of these immune cells to detect and destroy cancer cells, which has proven to be transformative for the treatment of B-cell malignancies[3–5]. While extending these successes to other types of cancers poses a range of challenges, many refinements to the basic CAR approach have now been achieved[6]. However, many applications exist for which an engineered T-cell receptor cannot be used to achieve the desired functionality, and thus additional sensing modalities are required[7].

Technologies for engineering customized cellular functions that respond to extracellular ligands—those that are not transported into the cytoplasm—enable cells to respond in defined ways to both the local environment and overall physiological state. Such approaches generally comprise engineering native receptors to confer responsiveness to new ligands[8–10] or coopting native receptor–signal transduction systems to drive induction of engineered signaling cascades[11] or gene circuits[12]. While the use of native pathways is facile and leverages the performance of components tuned through evolution, these approaches are also subject to regulation and crosstalk with other native cellular functions.

By contrast, orthogonal receptor systems may couple detection of extracellular ligands to engineered functions in a more programmable fashion. For example, synNotch receptors enable orthogonal detection of surface-bound extracellular ligands[13,14]. Each synNotch receptor comprises a core Notch domain flanked by modular extracellular and intracellular domains. Binding of a surface-bound ligand triggers protease-mediated cleavage and release of an exogenous transcription factor via a mechanism that requires ligand-binding-mediated mechanical forces, and thus synNotch receptors do not respond to soluble ligands. We recently developed a distinct self-contained receptor–signal transduction system, the modular extracellular sensor architecture (MESA)[15] (**Fig. 1a**), which is also orthogonal to native cellular pathways but is designed to enable the detection of soluble ligands. Each MESA receptor comprises two transmembrane chains—the target chain (TC) and the protease chain (PC). In this system, ligand-binding-induced dimerization of receptor extracellular domains promotes intracellular *trans*-cleavage of the target chain by the protease chain, which releases a sequestered engineered transcription factor into the cytoplasm. While this previous work demonstrated the feasibility of the MESA mechanism, ligand recognition was limited to detection of a model small-molecule analyte.

In this study, we investigated whether we could leverage the MESA design to generate a general platform for rewiring cellular functions in response to physiologically relevant cues. We evaluated strategies for incorporating both highly modular ligand-binding domains as MESA inputs and readily programmable transcription regulators as MESA outputs. By exploiting the modularity of the MESA design, this systematic investigation both elucidated the key factors impacting the performance of these novel receptors and ultimately validated a powerful, generalizable new technology for rewiring cellular input–output functions for therapeutic applications and as a tool for fundamental research.

RESULTS

VEGF-MESA receptor development

In this study, we systematically developed a generalizable strategy for engineering MESA receptors that sense physiologically relevant cues. To this end, we first investigated whether we could generate ligand recognition domains by coopting the single-chain variable fragments (scFvs) derived from monoclonal antibodies, which confer high-affinity ligand binding and are very stable[16]. scFvs have been developed against a wide range of antigens, providing a large pool of potential 'parts' for receptor engineering, and such domains have been used successfully in other engineered receptors such as CAR T cells[3–5] and synNotch receptors[13,14]. As a target analyte, we selected vascular endothelial growth factor (VEGF). VEGF promotes angiogenesis and is present at high levels in the tumor microenvironment in many cancers[17]. Monoclonal antibodies targeting VEGF have been developed as therapeutics[18,19], and several are well characterized structurally and biophysically[20,21]. Finally, VEGF is an attractive initial target for developing MESA receptors because this ligand is a homodimer (composed of two identical protein

[1]Department of Chemical and Biological Engineering, Northwestern University, Evanston, Illinois, USA. [2]Center for Synthetic Biology, Northwestern University, Evanston, Illinois, USA. [3]Chemistry of Life Processes Institute, Northwestern University, Evanston, Illinois, USA. [4]Member, Robert H. Lurie Comprehensive Cancer Center, Northwestern University, Evanston, Illinois, USA. *e-mail: j-leonard@northwestern.edu

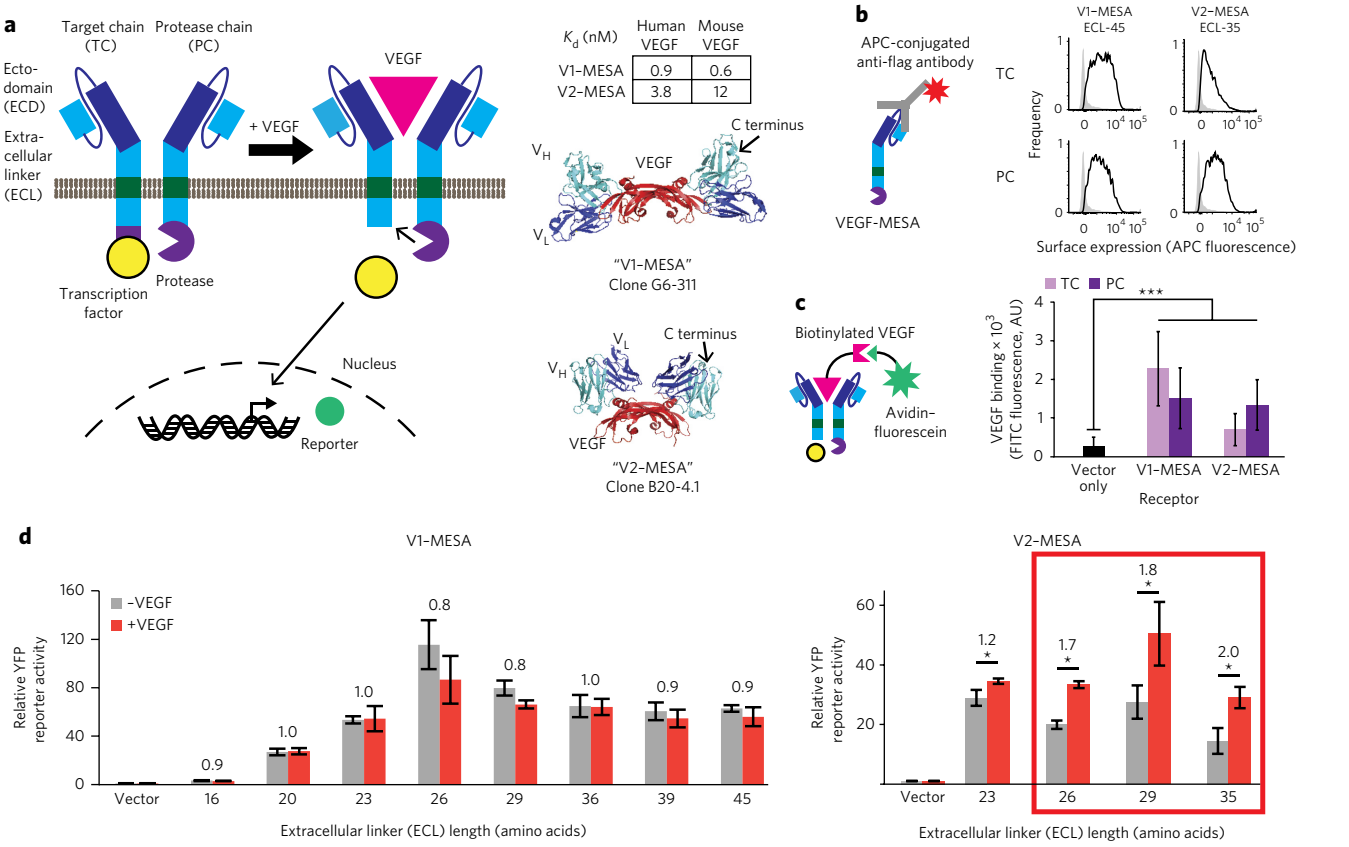

Figure 1 | VEGF-MESA receptor development. (**a**) Left, schematic of the VEGF-MESA mechanism, by which ligand-binding-induced dimerization results in *trans*-cleavage and release of a previously sequestered transcription factor. Right, crystal structures of two antigen-binding fragments (Fabs; blue and cyan indicate light-chain variable and heavy-chain variable domains, respectively, within each Fab) binding to each of two epitopes on VEGF (red)[20]. Table, reported equilibrium dissociation constants for Fabs binding to human and mouse VEGF[21]. (**b**) Cell-surface expression of representative VEGF-MESA constructs was evaluated by flow cytometry. Variants shown here differ in the lengths (in amino acids) of the non-structured extracellular linkers (ECL). Shaded regions represents vector-only transfected controls. At least 5,000 cells were analyzed for each condition, and this experiment is representative of two independent experiments. APC, allophycocyanin. (**c**) VEGF binding to VEGF-MESA was quantified using flow cytometry. Bar heights correspond to mean fluorescence intensities of samples comprising at least 5,000 transfected cells, and each error bar represents 1 s.d. This experiment is representative of two independent experiments. (**d**) VEGF-inducible signaling by VEGF-MESA was quantified by flow cytometry. "Reporter activity" was calculated by quantifying mean fluorescence intensity (MFI) of yellow fluorescent protein (YFP) in transfected cells, then normalizing this value to that calculated for the internal control (cells transfected with reporter only, the value for which was set to 1). The red box highlights constructs exhibiting significant VEGF-inducible signaling. Numbers above the bars represents fold induction, calculated by dividing the reporter signaling in the presence of VEGF by the reporter signaling in the absence of VEGF. Experiments were conducted in biological triplicate, each experiment is representative of at least three independent biological experiments, and error bars represent 1 s.d. (*$P \leq 0.05$, ***$P \leq 0.001$)

domains), such that any scFv that binds to VEGF could conceivably be engineered into MESA chains to confer ligand-binding-induced receptor dimerization.

To initially develop MESA receptors responsive to VEGF (VEGF-MESA), we used a general strategy to assess receptor design and functionality. We initially evaluated two different anti-VEGF scFv clones, which we termed G6 and B20 after the names of the monoclonal antibodies from which we derived these scFvs[21] (see Online Methods). These antibodies bind VEGF with different affinities and orientations, although each clone binds to the same face of VEGF[20,21] (**Fig. 1a**). We fused scFv clones G6 and B20 each to the extracellular portions of a MESA receptor scaffold (these constructs are hereafter termed V1–MESA and V2–MESA, respectively), including a range of flexible linkers $(Gly_2Ser)_x$ in between the scFv and transmembrane domain. The intracellular domains comprised a tobacco etch virus (TEV) protease on the PC, and the cognate cleavage sequence followed by an engineered transcription factor (tTA) on the TC, as in the initial MESA design[15]. We carried this receptor library forward for evaluation.

We first investigated whether VEGF-MESA receptors bound VEGF at the cell surface. When expressed in HEK 293FT cells, both V1–MESA and V2–MESA were expressed on the cell surface so long as the extracellular linker exceeded a minimal length of approximately 26 amino acids (**Fig. 1b**; **Supplementary Results**, **Supplementary Fig. 1a**). In our initial constructs, the TCs were expressed at the cell surface to a substantially greater extent than the PCs. Given that these two chains are identical on the extracellular face and transmembrane regions, we hypothesized that the inner membrane-proximal sequence on the PC may destabilize these proteins. To test this theory, we inserted the two membrane-proximal amino acids derived from the TC (which exhibited robust surface expression) into the same location on the PC, and, as predicted, this modification conferred robust surface expression of the PC (**Supplementary Fig. 2**). Therefore, we used such a linker for all PC constructs. All V1–MESA and V2–MESA expressed at the cell surface were capable of binding recombinant VEGF, and binding did not vary substantially with extracellular linker length beyond the minimum required to achieve cell-surface expression of the MESA

chains (**Fig. 1c**; **Supplementary Fig. 1**). Altogether, we discovered a subset of VEGF-MESA that was expressed on the cell surface and was capable of binding extracellular VEGF, and we carried this library forward for functional evaluation.

We next tested whether exposure to VEGF induced VEGF-MESA signaling. For V1–MESA, signaling in the absence of ligand increased as extracellular linker length increased from 16 to 30 amino acids, and lengthening linkers beyond this point led to no further increases in background signaling (**Fig. 1d**, left). Upon addition of VEGF, V1–MESA did not exhibit any ligand-inducible signaling at any linker length. The background signaling of V2–MESA was generally constant across all linker lengths evaluated and was consistently lower than the background signaling level conferred by V1–MESA (**Fig. 1d**, right). Most notably, for several V2–MESA configurations, we observed significant ligand-inducible signaling, with up to a two-fold increase in reporter output upon exposure to VEGF. This observation established the fundamental feasibility of engineering MESA receptors that sense exclusively extracellular cues.

We next evaluated how modifying the interchain cleavage kinetics might modulate VEGF-MESA signaling. Because we developed the initial intracellular VEGF-MESA architecture in order to limit background signaling in the absence of ligand[15], we hypothesized that altering the protease cleavage kinetics, by changing the final residue of the TEV protease cleavage sequence from methionine (M) to glycine (G) (which increases k_{cat} by ~50%[22]), could enhance signaling. VEGF-MESA with the G cleavage sequence were indeed expressed on the surface (**Supplementary Fig. 3a**) and bound recombinant VEGF (**Supplementary Fig. 3b**), but neither V1–MESA or V2–MESA bearing this cleavage sequence modification exhibited ligand-inducible signaling (**Supplementary Fig. 3c**). We inferred that for these G-cleavage-sequence MESA, transient diffusive encounters between the TC and PC resulted in cleavage and background signaling, thereby removing the dependence on the VEGF ligand to induce signaling. These results suggest a model wherein once one introduces a new ligand-binding modality, tuning MESA cleavage kinetics is neither necessary nor especially fruitful.

VEGF-MESA receptor implementation

Having developed a functional VEGF-MESA architecture, we next turned from protein engineering to investigate how to best implement such a receptor in order to achieve desirable performance characteristics. Such characteristics could include low background signaling in the absence of ligand and large fold induction upon ligand addition, and we hypothesized that there may be tradeoffs between these characteristics that depend on the manner in which the receptor is implemented. To frame this investigation, we posited that during the course of receptor expression, trafficking, and ligand binding, MESA receptors may enter a number of distinct complexes (**Fig. 2a**). Induction of signaling requires the formation of productive dimers, in which one TC and one PC dimerize at the cell surface to mediate *trans*-cleavage. However, since the ectodomains of both chains are identical, VEGF binding may also induce the formation of homotypic dimers in which two TCs or two PCs dimerize, which would not comprise functional signaling complexes. Moreover, it is also possible for TCs and PCs to encounter one another in the ER, secretory pathway, or cell surface, all of which would contribute to background signaling and generate 'dead' TCs that can subsequently act as competitive inhibitors of VEGF-induced MESA signaling. We hypothesized that each of these processes would render MESA performance dependent upon the rate(s) and ratio with which each receptor chain is expressed.

To investigate these questions, we systematically varied the expression of each MESA chain in a combinatorial fashion (**Fig. 2b**; **Supplementary Fig. 4a–d**). Signaling in the absence of ligand was quite low for all VEGF-MESA receptors, although background signaling diminished somewhat for low amounts of MESA plasmids. Most notably, for both V1–MESA and V2–MESA, we observed regimes that resulted in ligand-inducible signaling. Generally, we observed the greatest ligand-inducible signaling when TC:PC expression ratios were high, and within the signaling-competent regime, increasing TC expression levels enhanced both background and ligand-inducible signaling. Using these high-performing receptor expression conditions, we next investigated how VEGF-MESA signaling varied with VEGF dose (**Fig. 2c**). Interestingly, the dose–response curves for V1–MESA and V2–MESA were somewhat distinct. V1–MESA exhibited a substantial response to VEGF at doses as low as 25 ng/ml (**Fig. 2c**, left), whereas V2–MESA required a higher VEGF dose (150 ng/ml) to exhibit a substantial response (**Fig. 2c**, right). Moreover, V2–MESA exhibited a large dynamic range of differential responses to VEGF dose, whereas V1–MESA signaling reached a maximum at a relatively low concentration of VEGF. Possible contributors to such differences include ligand-binding affinity (V1–MESA is predicted to bind VEGF tighter than does V2-MESA; **Fig. 1a**) and differences between the geometric orientations in which ligand binding occurs (**Fig. 1a**). For the sake of comparability, we opted to use a VEGF dose of 250 ng/ml, the lowest concentration that resulted in maximal reporter induction for both V1–MESA and V2–MESA, for future analyses. Altogether, V1–MESA and V2–MESA responded to VEGF with different sensitivities and dynamic ranges, suggesting that these properties may be tuned based upon the desired application.

Since tuning MESA expression levels by varying plasmid dose may not be feasible for some applications, we also investigated a method for tuning expression by varying translation rates. To this end, we introduced synthetic elements into the 5′ UTR of MESA expression constructs, termed synthetic upstream open reading frames (uORF), to vary both the rate and frequency of translation initiation[23]. We screened a small library of these elements and observed that different uORF sequences did confer differential levels of MESA surface expression (**Supplementary Fig. 5a**,**b**). We used a uORF leading to high protein expression for the TC, and we co-transfected this plasmid at a 1:1 ratio with PC plasmids encoding a variety of uORFs. Interestingly, background signaling in the absence of ligand varied with uORF choice, following the same trend with which the level of MESA surface expression varied with uORF choice (**Supplementary Fig. 5c**). Moreover, multiple combinations of MESA receptors containing a variety of uORFs exhibited significant VEGF-mediated reporter induction. This result confirms that tuning the relative surface expression levels of the TC and PC can confer VEGF-inducible MESA signaling and that this tuning may be implemented via multiple strategies to achieve similar MESA performance.

Cellular rewiring via VEGF-MESAs

We next investigated whether we could modify the MESA output to regulate endogenous gene expression. To this end, we replaced tTA with a readily reprogrammable transcription factor based upon the CRISPR–Cas9 genome editing system (refs. 24–26). In this system, catalytically inactive Cas9 (dCas9) is genetically fused to the VP64 (ref. 27) transcriptional activation domain (dCas9–TF), and expression of dCas9–TF with a single-guide RNA (sgRNA) complementary to a genomic target leads to transcriptional activation of the target gene (**Fig. 3a**). As a proof of principle, we chose to target dCas9–TF to the human interleukin 2 (IL-2) gene for two main reasons. First, IL-2 performs diverse functions *in vivo*, including preserving peripheral immune tolerance by stimulating regulatory T cells, although high doses of IL-2 promote immune activation via simulation of cytotoxic T-cell proliferation[28]. Thus, achieving VEGF-induced expression of IL-2 is a non-natural cellular function that could be of use for immunotherapy. Second, transcription factors based upon transcription-activator-like effector (TALE) domains can reactivate the normally silenced IL-2 locus in HEK 293FT cells[29], such that this output comprises a suitable test of the proposed functional rewiring.

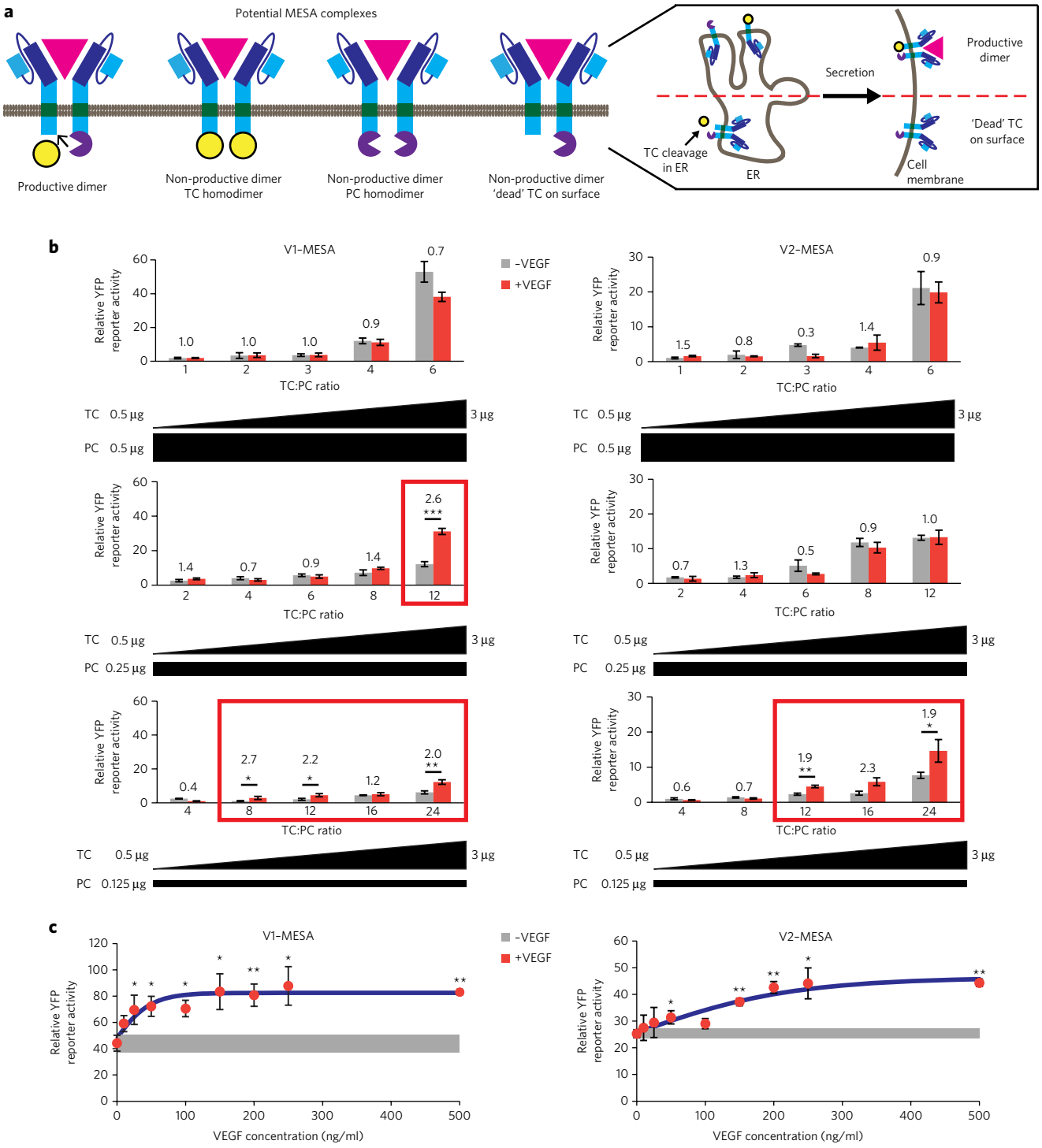

Figure 2 | VEGF-MESA receptor implementation. (**a**) This cartoon illustrates potential MESA complexes expected to form upon VEGF-binding-induced dimerization. The blowout at right illustrates the proposed mechanism by which 'dead' TC complexes may form as a result of transient receptor contact during trafficking or on the cell surface. (**b**) Both overall expression levels and ratios of the two VEGF-MESA chains were varied by dosing in different amounts of plasmid encoding each of the two MESA chains (TC and PC), as indicated in both the table (plasmid ratio) and ramps (plasmid masses) placed under each panel. Red boxes highlight the regimes in which VEGF-inducible receptor signaling was observed. Numbers above the bars represents fold induction and data were analyzed as described in **Figure 1**. (**c**) Dose–response curve of VEGF-MESA. Based upon results shown in **b**, VEGF-MESA chains were expressed at a TC:PC ratio of 24 (3 µg TC plasmid and 0.125 µg PC plasmid per well). Horizontal gray bars highlight the 0 ng/ml VEGF sample to which each test sample was compared, with the thickness indicating one s.d. Blue sigmoidal lines were added to guide the eye. Data were analyzed as described in **Figure 1**. (*$P \leq 0.05$, **$P \leq 0.01$)

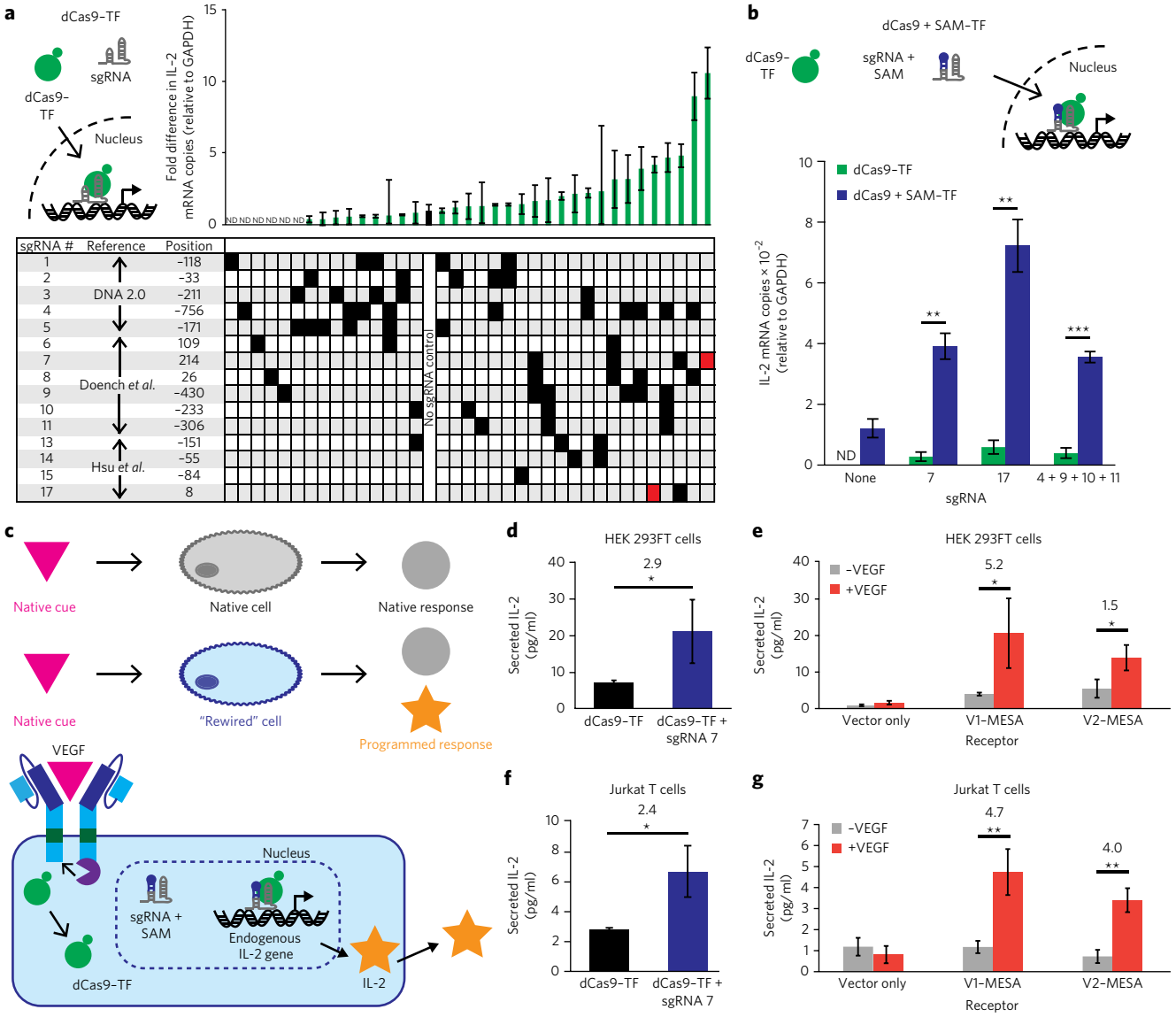

Figure 3 | Rewiring of cellular input-output using MESA. (**a**) Identification of sgRNAs that confer dCas9–TF-mediated induction of IL-2 expression. sgRNAs were screened individually and in combination with one another, and IL-2 mRNA expression was measured by qPCR. IL-2 mRNA copy number was normalized to GAPDH mRNA copy number, and this ratio was normalized to that calculated for cells transfected with only dCas9–TF (black bar). Red squares in the table indicate sgRNA that, individually, confer substantial IL-2 expression and were selected for further analysis. mRNA concentrations were evaluated in technical triplicate, and results are representative of three independent biological experiments. (**b**) Evaluation of SAM system[33] for enhancing dCas9–TF-induced IL-2 gene expression. Data were analyzed as in **a**. (**c**) This cartoon summarizes the proposed scheme for rewiring a cell to generate a non-natural function, whereby exposure to a canonically immunosuppressive cue (VEGF) results in the production of a canonically immunostimulatory factor in response (IL-2). (**d**–**g**) IL-2 secretion driven by soluble dCas9–TF was evaluated in HEK 293FT cells (**d**) and Jurkat T cells (**f**) and quantified by ELISA. VEGF-inducible secretion of IL-2 by cells expressing VEGF-MESA–dCas9–TF at a TC:PC ratio of 10 and sgRNA 7 was evaluated in HEK 293FT cells (**e**) and Jurkat T cells (**g**). Each sample was quantified in technical triplicate, and data shown are representative of three independent biological experiments (see **Supplementary Fig. 8**). Numbers above the bars represents fold induction, as described in **Figure 1**. Error bars represent 1 s.d. (*$P \leq 0.05$, **$P \leq 0.01$)

Since no previous studies had systematically evaluated sgRNAs for achieving dCas9–TF-mediated transcriptional activation of IL-2 in human cells, we first developed a library of sgRNAs targeted to a region spanning upstream and downstream of the IL-2 transcription start site (positions 800 to +250; see **Supplementary Fig. 6**) using three different *in silico* sgRNA design tools[30–32]. We coexpressed dCas9–TF with 15 different sgRNAs, either individually or in combination, in HEK 293FT cells, and we evaluated the induction of IL-2 mRNA expression by qPCR (**Fig. 3a**). Although many sgRNAs conferred minimal impacts on transcription, sgRNA 7 and 17 each individually resulted in significant induction of IL-2 transcription, as did several combinations of sgRNAs (five- to ten-fold more IL-2 transcription than was observed with dCas9–TF alone). We carried the most promising sgRNAs (7, 17, 4 + 9 + 10 + 11) forward for further investigation.

We next investigated whether recently reported methods for enhancing dCas9–TF-mediated transcription could be harnessed to enhance transcription from the endogenous IL-2 gene. To do so, we used the synergistic activation mediator (SAM) system[33], in which the sgRNAs were modified to contain three binding loops derived from the bacteriophage MS2 coat protein, and two transcriptional activators (p65 and HSF1) were fused to the MS2 protein (**Fig. 3b**).

Targeting IL-2 via SAM + dCas9–TF substantially enhanced transcription (10- to 15-fold) compared todCas9–TF alone (**Fig. 3b**), and thus we next evaluated SAM in the context of MESA.

Combining the functional components identified above, we next evaluated whether VEGF-MESA output could be redirected to induce transcription of endogenous IL-2 (**Fig. 3c**). First, we replaced the tTA domain of the TC with dCas9–TF (V1–MESA–dCas9–TF or V2–MESA–dCas9–TF) and confirmed that these constructs were expressed at the cell surface (**Supplementary Fig. 7**). To evaluate the functional performance of these receptors, we transfected V1–MESA–dCas9–TF or V2–MESA–dCas9–TF along with sgRNA 7 and SAM components into HEK 293FT cells, exposed cells to VEGF, and quantified IL-2 secretion (**Fig. 3e**; **Supplementary Fig. 8**). Monitoring IL-2 protein expression provides a robust, time-integrated metric of MESA output by circumventing potential artifacts associated with mRNA expression dynamics. We observed significant VEGF-induced IL-2 secretion for cells expressing either V1–MESA–dCas9–TF or V2–MESA–dCas9–TF, with the V1 receptor conferring a somewhat higher overall response (~20 pg/ml IL-2 protein) and a better fold induction (5.2-fold) compared to the V2 receptor. In the presence of VEGF, both V1–MESA and V2–MESA drove secretion of IL-2 at levels similar to those achieved by transient transfection of soluble dCas9–TF along with sgRNA 7 (**Fig. 3d**). Although sgRNA 17 drove high levels of IL-2 mRNA expression when coexpressed with the SAM components, transfecting sgRNA 17 in combination with V1–MESA or V2–MESA–dCas9–TF did not result in any VEGF-induced IL-2 secretion (**Supplementary Fig. 9a**). We do not yet have an explanation for this result, which was repeatable across multiple experiments. Further increasing the TC:PC ratio did not result in inducible signaling for either receptor (**Supplementary Fig. 9b**). Thus, the VEGF-MESA platform successfully conferred a novel, programmed functionality in HEK 293FT cells.

Finally, we investigated whether our MESA reprogramming strategy could be extended to rewire a distinct, physiologically relevant cell type. To this end, we chose to evaluate the Jurkat human T cell line, which is capable of secreting IL-2 but does not do so in response to VEGF[34]. V1–MESA–dCas9–TF and V2–MESA–dCas9–TF were expressed on the surface of Jurkat cells (**Supplementary Fig. 7**). We then transfected Jurkat cells with MESA chains, at the same TC:PC ratio used in HEK 293FT cells. We observed substantial VEGF-inducible secretion of IL-2 for both V1 and V2 receptors, and we did not observe IL-2 secretion in the absence of the MESA components (**Fig. 3g**; **Supplementary Fig. 8**). Furthermore, we confirmed that in the presence of VEGF, IL-2 accumulated only in transfected cells (**Supplementary Fig. 10**). As we observed in HEK 293FT cells, the V1 receptor again outperformed the V2 receptor in terms of both level of IL-2 secretion and fold induction, and when induced, each receptor drove secretion of IL-2 at levels comparable to those conferred by co-transfection of soluble dCas9–TF with sgRNA 7 (**Fig. 3f**). Notably, this observation represents the first functional rewiring of human immune cells to secrete an immune-potentiating molecule in response to an immunosuppressive cue, which is a response not observed in nature. Moreover, although we observed a lower IL-2 production level for Jurkat cells than for HEK 293FT cells, transfection efficiency of Jurkat cells was also substantially lower (~5% for Jurkat cells compared to 80% for HEK 293FT cells), and only the transfected Jurkat cells exhibited IL-2 accumulation (**Supplementary Fig. 10**). Taking this factor into account, we estimated the VEGF-induced production rate of IL-2 to be 5 pg IL-2/10^5 transfected cells/day for HEK 293FT cells and 15 pg IL-2/10^5 transfected cells/day for Jurkat cells, such that on a per=cell basis, functional rewiring may perform similarly in these two cell types. Altogether, these data demonstrate that the MESA platform comprises a generalizable synthetic biology technology for engineering cells to manifest novel, programmable, input–output functions that could be of use for both translational applications and fundamental research.

DISCUSSION

In this study, we developed a novel strategy for constructing customized cellular functions by functionally rewiring cellular input–output. Here, we consider key lessons learned in this investigation of MESA receptor design and implementation and suggest strategies for using this technology in future applications.

A central conclusion is that MESA's modular design and mechanism enabled the rational development of receptors that recognize novel inputs (soluble extracellular ligands). First, we considered the changes required to convert the original model MESA receptors, which signal in response to rapamycin-induced dimerization of the ectodomains[15], into MESA receptors that recognize physiologically relevant ligands. Achieving robust cell surface expression of MESA receptors using scFvs as ligand-binding domains required two key modifications: (i) inserting additional amino acids into the intracellular membrane-proximal portion of the PC and (ii) extending the non-structured extracellular linker between the transmembrane and scFv domains of each receptor chain. We hypothesize that both of these requirements may be interpreted as providing the geometric flexibility required to enable folding of all MESA domains. Notably, extending the extracellular linker domains beyond the minimum length required to achieve surface expression did not incur observable deficits in cell surface expression, ligand binding, or ligand-inducible signaling. This is consistent with prior observations made using the model MESA receptors, all of which confirm that, as intended, MESA signaling occurs via a mechanism by which ligand binding-induced dimerization of TC and PC mediates *trans*-cleavage by boosting the contact frequency between these chains, rather than by constraining these chains in a geometrically defined configuration that 'causes' *trans*-cleavage[15]. Therefore, we anticipate that MESA receptors incorporating novel scFvs need to include an extracellular linker of 'reasonable' length. Notably, the scFvs on the TC and PC must bind to non-overlapping epitopes on a single-ligand molecule, whether in a homotypic fashion, as was the case in this study, or in a heterotypic fashion. Moreover, the binding of the TC and PC to the analyte must bring the two chains together in a manner that enables the intracellular domains of these receptor chains to contact one another. The fact that both V1–MESA and V2–MESA exhibited ligand-inducible signaling supports the expectation that multiple geometries may meet this requirement, since the C termini of the V1 and V2 antibodies (which abut the flexible non-structured linkers) are separated by substantially different distances when bound to VEGF (85 and 100 Å separation, respectively[20]). For other scFv–ligand complexes, longer extracellular linkers may be required, and for other scFv–linker complexes in which scFvs are sufficiently separated in space when simultaneously bound to ligand, it might not be possible to accommodate both ligand binding and efficient signaling. In any event, the rules identified in this study provide relatively straightforward guidance as to how design-driven modifications may be used to efficiently evaluate novel receptor designs.

The modular nature of MESA design also enabled the straightforward implementation of novel receptor output (release of Cas9-based transcription factors). Since replacing tTA with dCas9–TF resulted in functional receptors with minimal adjustments, we did not identify specific challenges associated with substituting novel transcription factors into the intracellular domain of the TC. Interestingly, we observed a higher fold induction for VEGF-MESA based upon dCas9–TF compared to those based upon tTA. One likely explanation is that tTA- and TetO-based reporters are sensitive to low amounts of tTA (i.e., small amounts of transcription factor lead to moderate levels of reporter induction), which may be especially true in the context of transfection, in which many copies of the reporter exist in each cell. Conversely, dCas9–TFs are less potent, and thus high levels of dCas9–TF are required to drive robust transcription from endogenous genes[24]. Therefore, we hypothesize that the background level of TC cleavage by the PC may be comparable in

each receptor system and that differences in the sensitivities of the reporter genes to released transcription factors results in higher fold induction for the Cas9-based system as compared to the tTA-based system. We cannot exclude the possibility that some TFs may sterically occlude TEV-mediated cleavage of the target chain (suppressing ligand-inducible signaling) or that other TFs may confer less steric hindrance than either tTA or dCas9–TF (leading to higher ligand-independent background signaling). Overall, our observations suggest that MESA output may be diversified to accommodate at least a reasonably broad range of TF structures.

The manner in which a MESA receptor is implemented (i.e., expressed) also substantially affects functional performance, in part by impacting the balance between desirable and undesirable receptor complexes (**Fig. 2a**). Indeed, this statement is also true of natural receptor signaling—overexpression of natural receptors via transient or stable expression of transgenes can also lead to high background (ligand-independent) signaling. Although VEGF-MESA surface expression varied relatively little when changing either plasmid dose or the uORF used, we nonetheless observed substantial changes in MESA signaling both with and without ligand.

Ultimately, chromosomal integration of expression vectors may better enable tuning levels and distributions of MESA expression. Since lentiviral transgene expression varies greatly with integration site, stable expression of MESA chains from a single genomic landing pad may be a preferable strategy[35]. Notably, using the homotypic binding mechanism evaluated here, ligand binding may form PC–PC and TC–TC complexes, such that a maximum of 50% of the ligand-induced dimers are signaling competent. Using a heterotypic binding mechanism may circumvent this challenge, although maximizing ligand-inducible signaling would likely still require balancing TC and PC expression. Overall, implementing MESA receptors via the approaches reported here already achieved functional performance (for example, fold induction) that meets or exceeds that which has previously been observed with other engineered receptor systems[36]. Further exploring strategies for tuning expression within specific cellular contexts may improve functional performance without necessitating additional protein engineering.

Ultimately, rewiring cellular input–output may drive both translational applications and fundamental systems biology research. By enabling one to engineer cells that respond to a target extracellular cue via the expression of either transgenes (for example, tTA driven) or endogenous genes (for example, dCas9–TF-driven), MESA could facilitate the rapid implementation and evaluation of diverse therapeutic strategies. Additionally, the MESA platform could provide unique capabilities for fundamental research, particularly in the context of multicellular networks and whole organisms, including the ability to monitor, in a spatially and temporally resolved fashion, the presence (and perhaps concentration) of VEGF in a living animal. This information would complement that obtainable using existing reporter strategies, which could identify where the VEGF gene is being expressed but not where the VEGF protein accumulates in the extracellular environment. Furthermore, the MESA platform could complement genetic tools such as knockouts and knockins to enable the testing of novel hypotheses pertaining to multicellular network function. Thus, MESA comprises a powerful and generalizable technology in the mammalian synthetic biology toolbox, which expands our ability to build programmable cellular functions for myriad applications.

Received 31 May 2016; accepted 4 October 2016;
published online 12 December 2016

METHODS

Methods, including statements of data availability and any associated accession codes and references, are available in the online version of the paper.

References

1. Fischbach, M.A., Bluestone, J.A. & Lim, W.A. Cell-based therapeutics: the next pillar of medicine. *Sci. Transl. Med.* **5**, 179ps7 (2013).
2. Heathman, T.R. *et al.* The translation of cell-based therapies: clinical landscape and manufacturing challenges. *Regen. Med.* **10**, 49–64 (2015).
3. Porter, D.L., Levine, B.L., Kalos, M., Bagg, A. & June, C.H. Chimeric antigen receptor-modified T cells in chronic lymphoid leukemia. *N. Engl. J. Med.* **365**, 725–733 (2011).
4. Brentjens, R.J. *et al.* Safety and persistence of adoptively transferred autologous CD19-targeted T cells in patients with relapsed or chemotherapy refractory B-cell leukemias. *Blood* **118**, 4817–4828 (2011).
5. Kochenderfer, J.N. *et al.* B-cell depletion and remissions of malignancy along with cytokine-associated toxicity in a clinical trial of anti-CD19 chimeric-antigen-receptor-transduced T cells. *Blood* **119**, 2709–2720 (2012).
6. Fesnak, A.D., June, C.H. & Levine, B.L. Engineered T cells: the promise and challenges of cancer immunotherapy. *Nat. Rev. Cancer* **16**, 566–581 (2016).
7. Schwarz, K.A. & Leonard, J.N. Engineering cell-based therapies to interface robustly with host physiology. *Adv. Drug Deliv. Rev.* **105**, 55–65 (2016).
8. Pei, Y., Dong, S. & Roth, B.L. Generation of designer receptors exclusively activated by designer drugs (DREADDs) using directed molecular evolution. *Curr. Protoc. Neurosci.* **50**, 4.33.1–4.33.25 (2010).
9. Conklin, B.R. *et al.* Engineering GPCR signaling pathways with RASSLs. *Nat. Methods* **5**, 673–678 (2008).
10. Kalos, M. & June, C.H. Adoptive T cell transfer for cancer immunotherapy in the era of synthetic biology. *Immunity* **39**, 49–60 (2013).
11. Barnea, G. *et al.* The genetic design of signaling cascades to record receptor activation. *Proc. Natl. Acad. Sci. USA* **105**, 64–69 (2008).
12. Schukur, L., Geering, B., Charpin-El Hamri, G. & Fussenegger, M. Implantable synthetic cytokine converter cells with AND-gate logic treat experimental psoriasis. *Sci. Transl. Med.* **7**, 318ra201 (2015).
13. Morsut, L. *et al.* Engineering customized cell sensing and response behaviors using synthetic notch receptors. *Cell* **164**, 780–791 (2016).
14. Roybal, K.T. *et al.* Precision tumor recognition by T cells with combinatorial antigen-sensing circuits. *Cell* **164**, 770–779 (2016).
15. Daringer, N.M., Dudek, R.M., Schwarz, K.A. & Leonard, J.N. Modular extracellular sensor architecture for engineering mammalian cell-based devices. *ACS Synth. Biol.* **3**, 892–902 (2014).
16. Wörn, A. & Plückthun, A. Stability engineering of antibody single-chain Fv fragments. *J. Mol. Biol.* **305**, 989–1010 (2001).
17. Ferrara, N. VEGF and the quest for tumour angiogenesis factors. *Nat. Rev. Cancer* **2**, 795–803 (2002).
18. Ferrara, N., Hillan, K.J., Gerber, H.P. & Novotny, W. Discovery and development of bevacizumab, an anti-VEGF antibody for treating cancer. *Nat. Rev. Drug Discov.* **3**, 391–400 (2004).
19. Yang, J.C. *et al.* A randomized trial of bevacizumab, an anti-vascular endothelial growth factor antibody, for metastatic renal cancer. *N. Engl. J. Med.* **349**, 427–434 (2003).
20. Fuh, G. *et al.* Structure–function studies of two synthetic anti-vascular endothelial growth factor Fabs and comparison with the Avastin Fab. *J. Biol. Chem.* **281**, 6625–6631 (2006).
21. Liang, W.C. *et al.* Cross-species vascular endothelial growth factor (VEGF)-blocking antibodies completely inhibit the growth of human tumor xenografts and measure the contribution of stromal VEGF. *J. Biol. Chem.* **281**, 951–961 (2006).
22. Kapust, R.B., Tözsér, J., Copeland, T.D. & Waugh, D.S. The P1′ specificity of tobacco etch virus protease. *Biochem. Biophys. Res. Commun.* **294**, 949–955 (2002).
23. Ferreira, J.P., Overton, K.W. & Wang, C.L. Tuning gene expression with synthetic upstream open reading frames. *Proc. Natl. Acad. Sci. USA* **110**, 11284–11289 (2013).
24. Maeder, M.L. *et al.* CRISPR RNA-guided activation of endogenous human genes. *Nat. Methods* **10**, 977–979 (2013).
25. Perez-Pinera, P. *et al.* RNA-guided gene activation by CRISPR–Cas9-based transcription factors. *Nat. Methods* **10**, 973–976 (2013).
26. Gilbert, L.A. *et al.* CRISPR-mediated modular RNA-guided regulation of transcription in eukaryotes. *Cell* **154**, 442–451 (2013).
27. Sadowski, I., Ma, J., Triezenberg, S. & Ptashne, M. GAL4-VP16 is an unusually potent transcriptional activator. *Nature* **335**, 563–564 (1988).
28. Arenas-Ramirez, N., Woytschak, J. & Boyman, O. Interleukin-2: biology, design and application. *Trends Immunol.* **36**, 763–777 (2015).
29. Anthony, K., More, A. & Zhang, X. Activation of silenced cytokine gene promoters by the synergistic effect of TBP-TALE and VP64-TALE activators. *PLoS One* **9**, e95790 (2014).
30. DNA2.0. CRISPR gRNA design tool https://www.dna20.com/eCommerce/cas9/input (2014).
31. Doench, J.G. *et al.* Rational design of highly active sgRNAs for CRISPR–Cas9-mediated gene inactivation. *Nat. Biotechnol.* **32**, 1262–1267 (2014).
32. Hsu, P.D. *et al.* DNA targeting specificity of RNA-guided Cas9 nucleases. *Nat. Biotechnol.* **31**, 827–832 (2013).

33. Konermann, S. *et al.* Genome-scale transcriptional activation by an engineered CRISPR–Cas9 complex. *Nature* **517**, 583–588 (2015).
34. Kotb, M., Majumdar, G., Tomai, M. & Beachey, E.H. Accessory cell-independent stimulation of human T cells by streptococcal M protein superantigen. *J. Immunol.* **145**, 1332–1336 (1990).
35. Duportet, X. *et al.* A platform for rapid prototyping of synthetic gene networks in mammalian cells. *Nucleic Acids Res.* **42**, 13440–13451 (2014).
36. Antunes, M.S. *et al.* Programmable ligand detection system in plants through a synthetic signal transduction pathway. *PLoS One* **6**, e16292 (2011).

Acknowledgments

K.A.S. and N.M.D. were supported in part by the National Institutes of Health T32 Training Grant GM 008449 through Northwestern University's Biotechnology Training Program. T.B.D. was supported by the Department of Defense (DoD) through the National Defense Science & Engineering Graduate Fellowship (NDSEG) Program. This work was supported by the Northwestern University Flow Cytometry Facility and a Cancer Center Support Grant (NCI CA060553). This project was supported by the Defense Advanced Research Projects Agency, Award number W911NF-11-2-0066 (to J.N.L.). No funding sources had any involvement in the writing of this manuscript.

Author contributions

K.A.S. performed, designed, and analyzed experiments. T.B.D. performed and analyzed experiments. K.A.S., N.M.D., and J.N.L. conceived of the study. K.A.S., T.B.D., and J.N.L. wrote the manuscript and prepared the figures.

Competing financial interests

The authors declare competing financial interests: details accompany the online version of the paper.

Additional information

Any supplementary information, chemical compound information and source data are available in the online version of the paper. Reprints and permissions information is available online at http://www.nature.com/reprints/index.html. Correspondence and requests for materials should be addressed to J.N.L.

ONLINE METHODS

DNA construct sources and engineering. Anti-VEGF scFvs and corresponding signal sequences were designed based upon the sequences of monoclonal antibodies raised against VEGF[37], the sequences of which were generously shared by G. Fuh (Genentech) (**Supplementary Note**). Interchain linkers of 15 non-structured amino acids were used to generate scFvs with strong preference for forming monovalent binding domains rather than higher-order complexes[38]. These genes were synthesized (Invitrogen) and cloned into an expression vector using previously characterized MESA parts[15]. The extracellular linker (ECL) library for V1 and V2-MESA was created using PCR (**Supplementary Table 1**), digesting the product with NheI and AgeI and inserting it back into the original backbone. The development of the tTA-responsive YFP reporter plasmid was described previously[15]. Source plasmids for Cas9 components included lenti dCAS–VP64_Blast (Addgene; #61425), lenti MS2–P65–HSF1_Hygro (Addgene; #61426), lenti sgRNA(MS2)_zeo backbone (Addgene; #61427) (ref. 33), MLM3636 (Addgene; #43860), and pMLM3705 (Addgene; #47754) (ref. 24). dCas9–VP64 (referred to here as dCas9–TF) was cloned into the MESA TC backbone in place of tTA using PCR (**Supplementary Table 1**), and the product was digested with NotI. sgRNAs were developed using overlapped primers (**Supplementary Fig. 4**), which were inserted into either the MLM3636 or lenti sgRNA(MS2) backbone digested with BsmBI. Sequences of all DNA plasmids and primers are in **Supplementary Table 1** and **Supplementary Note**.

Cell culture and transfection. HEK 293FT cells (Life Technologies/Thermo) and Jurkat cells (ATCC TIB-152) were maintained at 37 °C and 5% CO_2. HEK 293FT cells were cultured in Dulbecco's modified growth medium and Jurkat cells were cultured in RPMI-1640 (Life Technologies), each supplemented with 10% FBS, 1% penicillin–streptomycin, and 2 mM L-glutamine (Life Technologies). For HEK 293FT cells, transfections were performed in 6-well plates seeded at 7.5×10^5 cells in 2 ml media (immunohistochemistry and RNA experiments) or 24 well plates seeded at 1.5×10^5 cells in 0.5 ml media. 6–8 h post-seeding, cells were transfected using the $CaCl_2$–HEPES-buffered saline (HEBS) method with a total DNA content of 1–2 μg DNA per ml of media. All experiments included a plasmid expressing *Discosoma* sp. red fluorescent protein (DsRed) or blue fluorescent protein (BFP) as a control to assess transfection efficiency. For functional experiments, 12 h post-transfection, recombinant mouse VEGF-164 (BioLegend, carrier-free) was added to cells upon media change. For Jurkat cells, transfections were performed in 6-well plates seeded at 5×10^5 cells in 2 ml media. These cells were transfected using Lipofectamine LTX with Plus Reagent, as per manufacturer's instructions. For intracellular staining of IL-2, VEGF was added 24 h post-transfection in combination with 10 μg/ml brefeldin-A (Life Technologies).

Flow cytometry, reporter assays, and immunolabeling. Adherent cells were suspended in PBS with 2 mM EDTA (PBS–EDTA) and 5% bovine serum albumin (flow buffer). Suspension cells were washed into the same flow buffer. Approximately 1×10^4 single, live cells from each sample were analyzed using a LSRII flow cytometer (BD Biosciences) running FACSDiva software. Data were compensated and analyzed using FlowJo Software (Tree Star). Live, single cells were gated on the basis of scatter and transfected cells were gated on the basis of the presence of a DsRed or BFP transfection control for all experiments. "Reporter activity" was calculated as described in the caption of **Figure 1**. For immunolabeling on the cell surface, 1×10^6 cells were harvested and subsequently labeled with 0.5 μg allophycocyanin (APC)-conjugated anti-Flag (anti-DDDDK) tag antibody (Abcam; #ab72569) for 30 min at 4 °C, and washed 3 times with flow buffer before analysis by flow cytometry. For intracellular staining of IL-2, cells were first fixed and permeabilized with 4% paraformaldehyde (Sigma) for 20 min at 4 °C, and then cells were resuspended in PBS with 0.2% BSA and 0.5% saponin (Sigma). Immunolabeling with 5 μl of an anti-IL-2 antibody (Thermo; RHCIL205) was performed as described for surface staining.

Statistical analysis. For most statistical analyses, two-tailed Student's *t*-tests were used. This test was chosen to evaluate whether a significant difference exists between two groups of samples, and the reported comparisons meet the two requirements of this test: (1) the values compared are expected to be derived from a normal distribution, and (2) the variance of each group is expected to be comparable to that of the comparison group, since the same transfection methodologies and data collection methods were used for all samples that were compared. A P value of ≤0.05 was considered statistically significant. To specifically evaluate whether two flow cytometry distributions were significantly different (i.e., **Figure 1c**), a chi-squared test was applied, with a significance threshold of $P < 0.05$.

VEGF binding assays. VEGF binding assays used the VEGF Biotinylated Fluorokine Kit (R&D Systems) as per the manufacturer's instructions. Briefly, 4×10^6 cells were harvested, incubated with biotinylated recombinant human VEGF and avidin–FITC reagents, washed to remove excess reagents, and finally resuspended in flow buffer before flow cytometry analysis.

Endogenous gene expression assays. RNA was isolated using Trizol (Life Technologies), and total RNA content was determined using a NanoDrop 2000 Spectrophotometer (Thermo Scientific). 500 ng of RNA was used for cDNA synthesis using the qScript cDNA synthesis kit (Quanta Biosciences). 2 μl of cDNA was mixed with 12.5 μL iQ SYBR Green qPCR supermix (Bio-Rad Laboratories), forward and reverse primers at a final concentration of 0.05 μM, and water to a final volume of 25 μl. qPCR reactions were run on a CFX Real-Time PCR Detection System (Bio-Rad Laboratories). All samples were quantified in technical triplicate using IL-2 and GAPDH primers. The quantification cycle (C_q) values were averaged for each primer set and the "no reverse transcriptase" control was subtracted from the mean. IL-2 and GAPDH standard curves were used to convert from C_q values to mRNA copies, and IL-2 values were subsequently normalized by the corresponding GAPDH values.

Protein secretion assays. Secreted IL-2 was quantified in supernatant using the Ready-Set-Go! IL-2 ELISA kit (eBiosciences) by following the manufacturer's instructions. Undiluted supernatant was assayed in technical triplicate and a BioTek Synergy H1 plate reader was used to analyze the resulting signal. Each sample was zeroed by subtracting the absorbance at 570 nm from absorbance at 450 nm, and a standard curve was used to convert between zeroed absorbance and protein concentration.

37. Lee, C.V. *et al.* High-affinity human antibodies from phage-displayed synthetic Fab libraries with a single framework scaffold. *J. Mol. Biol.* **340**, 1073–1093 (2004).
38. Atwell, J.L. *et al.* scFv multimers of the anti-neuraminidase antibody NC10: length of the linker between VH and VL domains dictates precisely the transition between diabodies and triabodies. *Protein Eng.* **12**, 597–604 (1999).